A FERROGRAPHIC STUDY OF BRONZE AND CAST IRON PLAIN BEARINGS

A. D. Sarkar*

Department of Mechanical Engineering,
University of Petroleum & Minerals,
Dhahran - 31261, Saudi Arabia

الخلاصـــة :

تمّ تعيين التآكل الميكانيكى للبيرنج (المَحْمِل) بواسطة الفروجرافي . وأعطى البيرنج (المَحْمِل) المحتوي على البرونز نقاط كثيرة مبعثرة وذلك عند رسم الحد (A_L) الأقصى للمساحة مع الأحمال والسرعات . وظهر أنّ هذه البعثرة تقلّ ، وتكون النتائج منسجمة مع بعضها عند استعمال المَحْمِل المصنوع من الحديد الزهر . لقد أعطى كلٌ من دليل التآكل الميكانيكي والمساحة أسفل المنحنى اتجاهاً مشابهاً كما في A_L ، لأن البارامتر (المَعْلَم) قد يكون كافٍ أثناء مراقبة الماكينة .

وتزيد A_L مع السرعة ولكنها قد تقل مع الحمل . ويحتمل أن يكون السبب ناتجاً عن تفتيت الجُزيئيات المتآكلة عند السطوح المتداخلة .

ونستنتج من ذلك أنه عندما تعمل الماكينة بسهولة ، فإن قيمة A_L تبقى فى حدود معينة . وفي حالة عدم عمل الماكينة بسهولة فإنه يلاحظ أن قيمة A_L تستمر في الارتفاع مع ازدياد الحمل ، ويكون هذا تحذيرا ببدء الإنهيار .

ABSTRACT

Wear of plain bearings was evaluated by ferrography. A bronze bearing gave a lot of scatter when the maximum percentage area, A_L, was plotted with loads and speeds. The scatter diminished and results were more consistent when cast iron bearings were used. The wear index and the area under the curve gave similar trends as A_L and hence the latter parameter may be sufficient while condition monitoring a machine. A_L increases with speed but can decrease with load, possibly, as a result of comminution of the wear particles at the interface. It is concluded that when a machine runs smoothly, the A_L values remain within a range. If the machine is in distress, the A_L values continue to rise with load, thus warning of incipient failure.

*Address for correspondence :
UPM Box No. 1953
University of Petroleum & Minerals
Dhahran - 31261
Saudi Arabia

A FERROGRAPHIC STUDY OF BRONZE AND CAST IRON PLAIN BEARINGS

NOTATION

A	=	Percent of particles on a ferrogram.
A_L	=	Percent area of large particles on a ferrogram.
A_S	=	Percent area of small particles on a ferrogram.
$A_L + A_S$	=	Total wear.
$A_L - A_S$	=	Severity of wear.
I_S	=	Wear Index = $A_L^2 - A_S^2$
V	=	Total volume of wear.
x	=	Distance along a ferrogram.
AUC	=	Area under the curve obtained by plotting A against x.
Y_L	=	Maximum value of the number of clusters per mm.
h_L	=	Maximum value of the thickness of clusters per mm.
N_L	=	Maximum value of the number of clusters per mm.
σ_y	=	Yield stress of the metal which is wearing.
S	=	Sliding distance.
K	=	Probability factor.
W	=	Applied load.
v	=	Surface speed.
t	=	Time.

INTRODUCTION

Decades ago, the oiler carried out his own maintenance, but modern machines are compact and it is not possible to examine the state of the surfaces of friction couples without expensive dismantling of parts. Experience shows, however, that the wear debris from machines exhibits a range of sizes and shapes, and that the size, in particular, reflects certain service conditions such as load and speed. For example, if the load and speed are excessive, large flake-like particles are expected from sliding components. Since the lubricating oil carries the wear product, extraction of the latter from an oil sample and subsequent examination of the debris should provide a technique for condition monitoring of industrial mechanisms. A method widely used in examining oil samples from machines is spectroscopy [1]. However, one serious shortcoming of the technique is that large particles cannot be detected [2], the upper limit being 1 μm [3]. Aircraft monitoring is carried out by spectroscopy [4] but there is a lack of confidence in this [5] and also in such techniques as magnetic plug sampling and oil filter analysis.

FERROGRAPHY

The ferrographic method of particle examination is being used increasingly largely because the shape and size of the wear debris can be established. Essentially, wear particles from a lubricating oil are deposited on a slide by magnetic means and the particles examined under a bichromatic microscope called a Ferroscope. It has been reported [6] that, in aeroengines, there can be as many as 10^{12} particles per ml in an oil sample. The metallic debris can be as long as 15 μm with thicknesses of the order of 1 μm at moderate loads [7, 8]. Among other forms, the shapes of the particles can be lath-like or spherical [9, 10].

The instrument used in this investigation was the analytical ferrograph. This gives two types of readings: A_L and A_S. A_L gives a measure of the size of the large particles, and A_S, that for the smaller particles.

From these parameters,

$$\text{The total wear} = A_L + A_S \quad (1)$$

$$\text{Severity of wear} = A_L - A_S \quad (2)$$

A Wear Index, I_S is defined as

$$I_S = A_L^2 - A_S^2 \quad (3)$$

The A_L and A_S values are measured by the ferroscope and they have been shown to correlate with other methods of wear evaluation. However, the correlation of ferrographic parameters with either the amount of wear or other techniques of condition monitoring is by no means definite [11]. For example, I_S correlates with the iron content as analyzed by Atomic Absorption Spectroscopy only when service variables are not altered at random and the wear rate is steady [12]. Ferrography has been used successfully in monitoring diesel engine wear [13] but becomes inadequate for mining machinery [14].

One suggestion [15] is that the total volume V of the particles with various sizes can be computed over the whole length of the ferrogram, which is 60 mm.

$$\text{Thus } V = K\int_0^{60}[h(x)A(x)]\,dx \qquad (4)$$

where $h(x)$ and $A(x)$ are, respectively, the thickness and percentage area of the deposit at a distance x, and K is a constant.

An estimate of the volume can also be obtained by plotting A against various positions on the ferrogram and then measuring the area under the curve, termed AUC.

EXPERIMENTAL METHODS

In these experiments, an attempt was made to observe the tribological behavior of plain journal bearings subjected to various loads and surface speeds by examining oil samples with the aid of ferrography. There were two bearing materials: a leaded bronze and a cast iron.

The Twin Bearing Rig

The arrangement of one bearing is shown in Figure 1 schematically. The test bearing assembly is in the center. A hard steel sleeve is mounted on the drive shaft and is so located with the aid of distance pieces that the bearing is in contact with it only. That is, the friction couple comprises a plain bearing and a hard steel sleeve.

Table 1. Composition and Treatment of Bronze Bearing to BS 1400, LB1 Specification.

Element	Weight Per Cent
Cu	Remainder
Sn	9.53
Zn	0.81
Pb	17.20
P	0.11
Ni	1.61
Fe	-
Al	-
Sb	0.60
Si	0.03

Hardness : 90 BHN. Treatment : Cast in shell moulds; Machined.

Table 2. Composition and Treatment of the Grey Cast Iron.

Element	Weight Per Cent
TC	3.21
Si	2.28
Mn	0.75
S	0.10
P	0.30

Hardness : BHN 230. Treatment : Sand Cast and Machined.

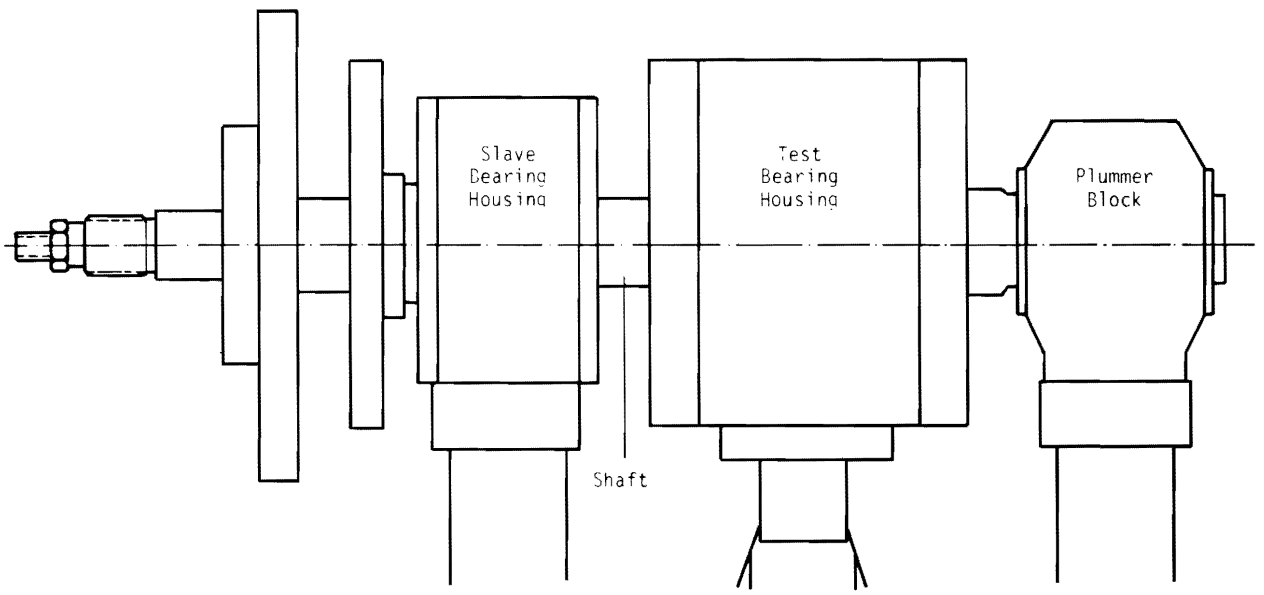

Figure 1. A General Sketch of the Bearing Rig Showing the Position of the Test Bearing.

A	56.6387-55.6514
B	50.0558-50.0685
C	35.0012-35.0266

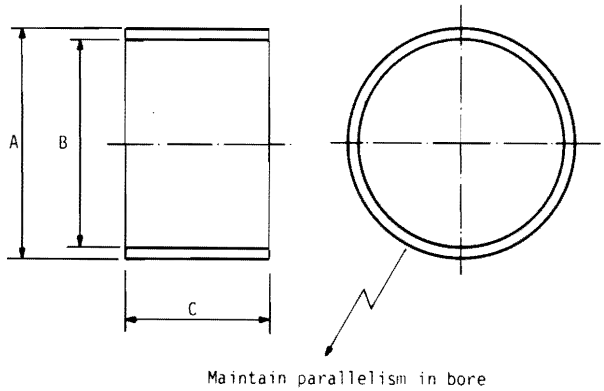

Figure 2. Nominal Dimensions of Test Bearing, mm.

The dimensions of the bearing and sleeve are shown in Figure 2 and 3 respectively. The compositions and treatments of the bearings and sleeves are given in Table 1, 2, and 3. The sleeves were quenched in water and tempered. They were ground to give an average CLA of 0.80 μm. The bronze bearings were used in the as-cast condition. The cast iron bearings were machined. The sleeves were always ground such that an annular gap of 0.0476 mm was maintained between a sleeve and the corresponding bearing.

Table 3. Composition and Treatment of the Steel Sleeve

Element	Weight Per Cent
C	1.1
Ni	0.28
Cr	1.20
Mo	0.09

Hardness : 910 HV. Treatment : Austenitized at 850°C; Quenched in cold water; Tempered at 120°C; Ground finished.

The torque arm arrangement is shown in Figure 4. The torque bar, A, is screwed to the test bearing and, due to frictional movement, it presses against a load cell. The load cell is calibrated to provide readings for the frictional force, F, so that for an applied load W, the coefficient of friction, $\mu = F/W$. The oil inlet and outlet temperatures, the temperature of the environment of the bearing housing and that of the mid-outer surface of the bearing are displayed continuously.

The Ferrogram

A ferrogram is produced by diluting the oil sample under investigation with a solvent and then pumped by a peristaltic pump onto a perspex slide. In these experiments 3 ml of oil was diluted with 1 ml of solvent. The slide is inclined and, as the oil flows down, the particles in it are subjected to a strongly increasing magnetic field. The magnetic field and the

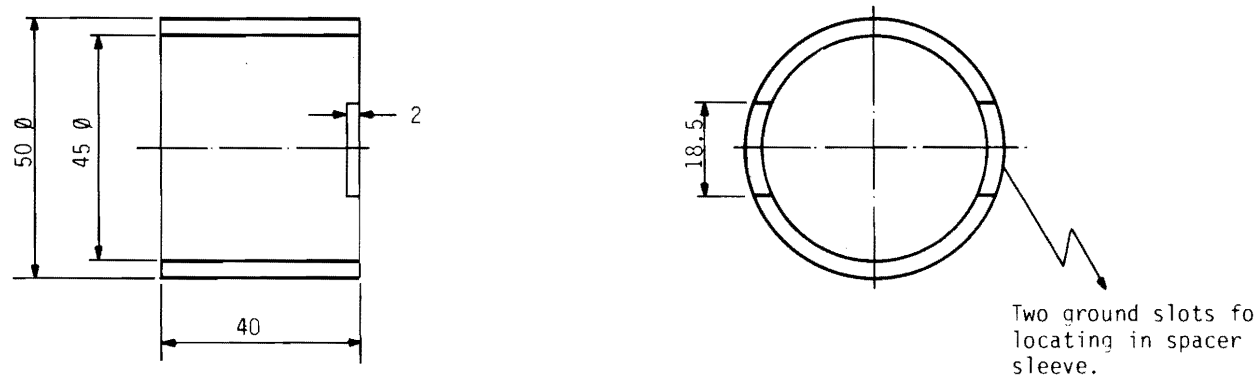

Figure 3. The Shaft Sleeve, the Journal Component, Showing Nominal Dimensions, mm.

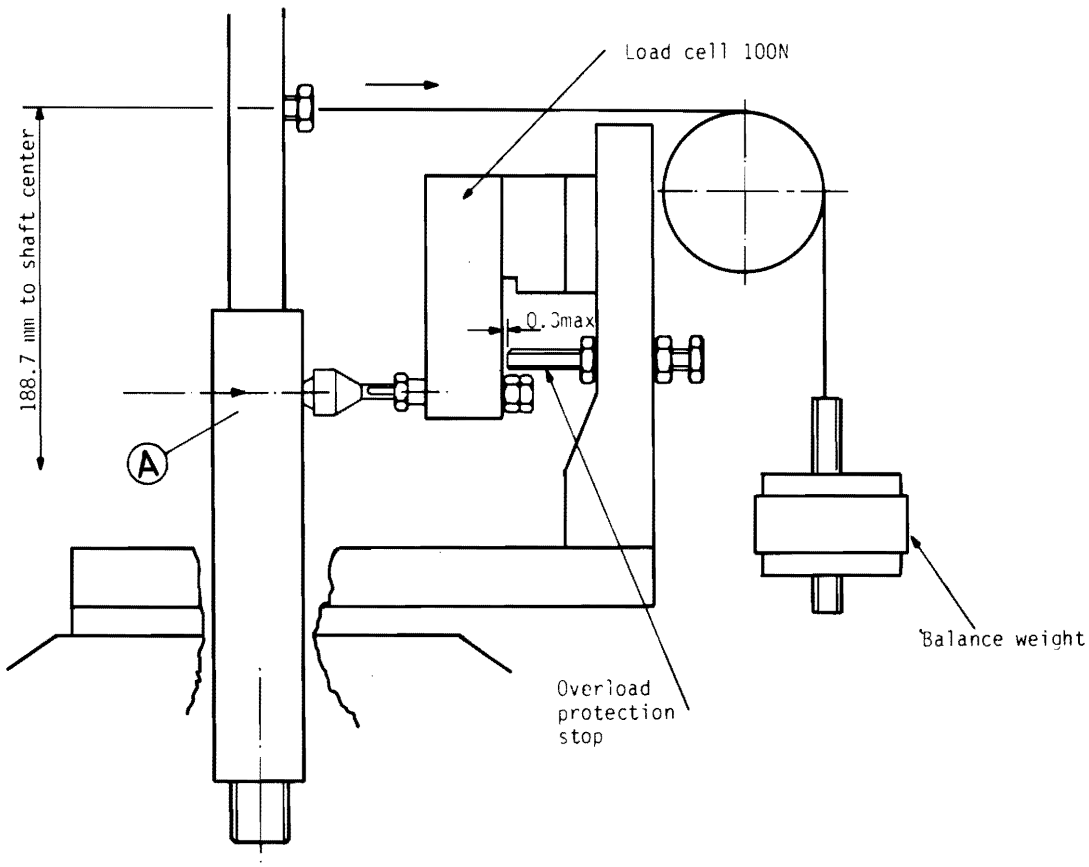

Figure 4. Torque Arm Arrangement.

drag force together cause the large particles to deposit at the upper end. The smaller particles settle further down at greater distances from the entry end. Once the oil is pumped completely, a washing and fixing treatment makes the particles adhere to the slide.

Measurement of A_L and A_S

The ferrogram is examined under the ferroscope which reads the optical density of the wear product with the aid of a densitometer. Thus the proportion of light blocked increases with an increase in the size of the wear particles, giving a high density reading. This attenuation of light appears as a digital display on the ferrogram reader. These readings are designated as A in this paper; A is actually the percent area of the slide covered by particles.

The Lubricating Oil

The oil used was a motor oil, whose specification is given in Table 4. A clean bearing and a sleeve were mounted and 1 liter of oil from the tank was made to flush the pipes, bypassing the bearing. The tank was then topped up with 1 liter of fresh oil and the lubricant was circulated through the bearing system for one hour. The motor was then started and, once the desired rpm was established, the load was applied. This was regarded as the zero time for the bearing trial. The oil flow rate was maintained at 20 ml min^{-1}.

Sampling

Initially oil samples were taken from various locations but, eventually, it was decided to withdraw samples from the middle of the tank as this gave similar ferrographic readings to samples from other positions and was the most convenient.

In a few trials, sampling was carried out at regular intervals and ferrograms prepared. It was observed that the A_L and A_S values increased steadily with time and became consistent in about 22 hours. It was decided to run each trial for 70 hours. This allowed time for dismantling and reassembling the bearing rigs so that one trial per bearing rig could be carried out in a week.

Table 4. Test results from oil samples : Leaded Bronze Bearings.

Properties	Sample No.					
	0*	1	2	3	4	5
Sp. Gr. at 260°F	0.8930	0.8964	0.8939	0.8928	0.8933	0.8938
Flash Point °F	435	405	415	425	420	405
Pour Point	15	15	20	20	15	15
Kinematic Viscosity at 100°F, cst	198.0	204.5	201.3	202.0	198.7	195.3
Sybolt Viscosity at 100°F sus	910	937	932	936	920	905
Kinematic Viscosity at 210°F cst	20.7	22.0	21.9	21.7	21.1	20.8
Sybolt Viscosity at 210°F sus	103.1	107.0	106.1	105.4	103.2	101.2
Viscosity Index	135	139	141	138	135	135

* Samples Nos. : 0 unused oil; 1 ≡ 3 kN, 1500 rpm; 2 ≡ 4.5 kN, 1500 rpm; 3 ≡ 6 kN, 1500 rpm; 4 ≡ 1.5 kN, 2500 rpm; (5 ≡ 6.0 kN, 2500 rpm, Cast Iron Bearing)

The Choice of Bearing Materials

The reason for choosing the bronze bearings was that some claim that nonferrous particles, if rubbed against steel, pick up the counterface material and hence can be trapped in a ferrogram. It was important, therefore, to verify this since many industrial machines use bronze plain bearings.

A few steel bearings were tried but they tended to seize quickly. It was therefore decided to use a set of flake graphite cast iron bearings to compare the ferrographic parameters with those from bronze.

Properties of Used Oil

Since particle concentration should increase with time, it was decided to make a record of the properties of the used oil from the tank. The oil samples were taken at the end of a trial and when the machine was still running. The results are given in Table 4.

Wear Metal Analysis

Samples from the bearing trials were analysed by AA spectroscopy but the results are not reported here because no correlation was found between ferrographic parameters and, say, the iron content of the wear product.

RESULTS FROM BRONZE BEARINGS

A-D Curve

A typical plot of percentage area covered A, against D, the distance in mm from the exit end of the ferrogram is shown in Figure 5. The A_L value is just beyond D = 50 mm in this case and the A_S is just beyond D = 10 mm. The area under the curve, AUC, is the area enclosed by the dotted lines and, in these experiments, includes the value of A_L and A value up to 40 mm towards the exit end.

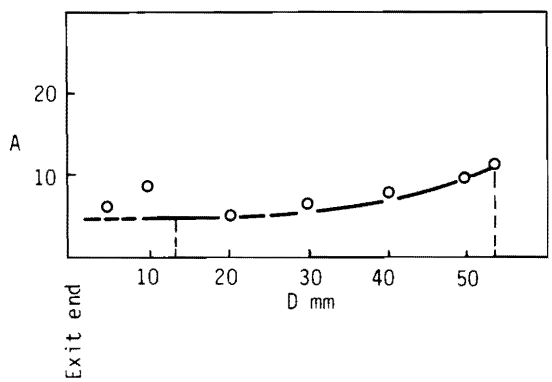

Figure 5. Variation of Percent Area, A, Covered with D, the Distance Along the Ferrogram from the Exit End. Bronze Bearings 0.6 kN; 500 rpm.

A_L vs. Load and Speed

For the leaded bronze bearings, the A_L values are plotted against the applied load at speeds of 500, 1000, 1500, and 2500 rpm respectively in Figure 6. The data show scatter but at the highest speed of 2500 rpm, the percent area covered decreases with load. If the A_L values are plotted against the rpm at various load (Figure 7), a trend can be noted. The higher the surface speed, the greater is the particle size.

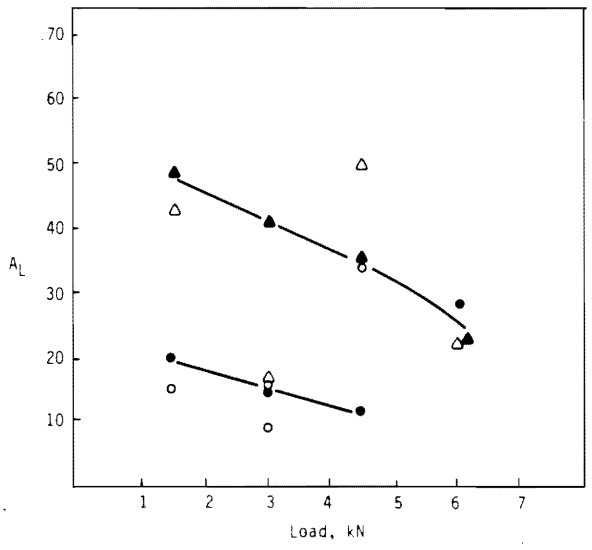

Figure 6. Variation of Maximum Per Cent Area, A_L, Covered, with Load at Various Speeds. Bronze Bearings; rpm ○ 500; △ 1000; ● 1500; ▲ 2500.

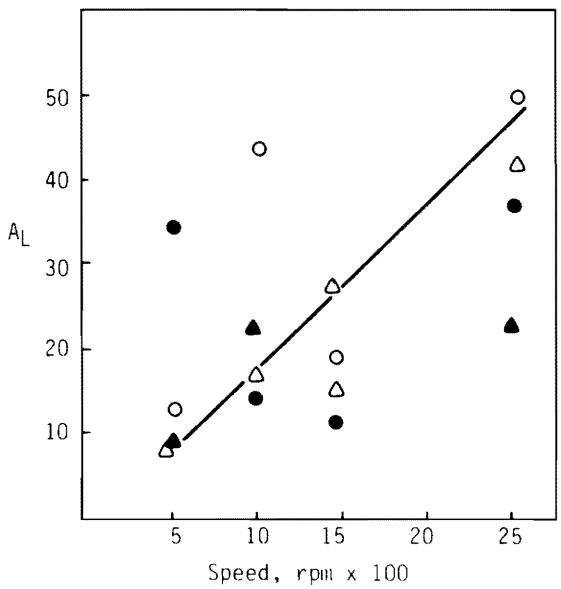

Figure 7. Variation of A_L with Speed at Various Loads. kN : ○ 1.5; △ 3.0; ● 4.5; ▲ 6.0.

A Measure of Volume

A ferrogram can measure the width, y, thickness, h, and the number, N, of the cluster-like deposits of wear debris per mm. The maximum values of these, designated as Y_L, h_L and N_L were chosen for correlation with service variables.

The results are not plotted here but considerable scatter was noted when Y_L, h_L and N_L were plotted individually against load. If, however, the product $h_L Y_L$ is plotted against load, declining values of the former are noted (Figure 8) as the load is increased but only at the highest speed of 2500 rpm. The trend is similar to that in Figure 6.

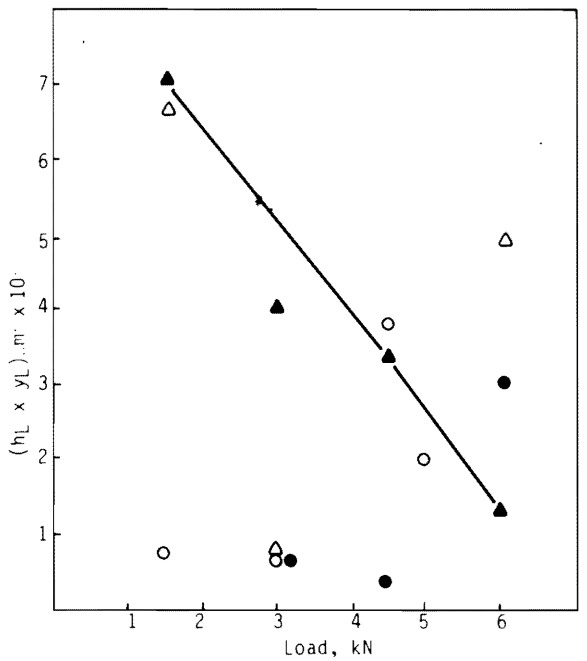

Figure 8. Variation of $(h_L \times y_L)$ with Load. Bronze Bearings.

Bearing Temperature

Whereas the bearing surface temperature, as measured by the thermocouple, was not very sensitive to applied load, it definitely showed significant increases as the speed of the machine was raised. Figure 9 shows the trend for A_L is to increase with increasing bearing temperature.

Coefficient of Friction

Although there were cases where a high value of the coefficient of friction showed a large value of A_L, there was considerable scatter and the results are not shown here.

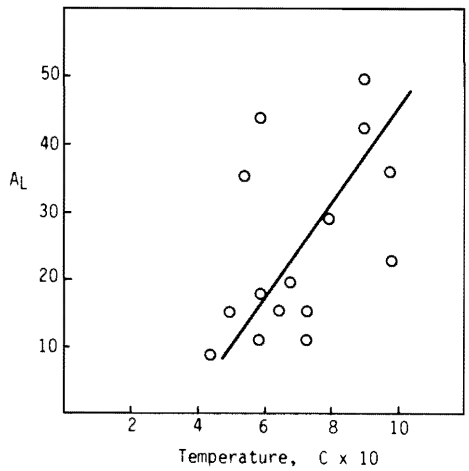

Figure 9. Variation of A_L with Bearing Temperature. Bronze Bearings.

Wear Index

The wear index (equation 3) shows a similar trend against load as that given by A_L (Figure 6). However, in a plot against speed or bearing surface temperature, scatter becomes considerable.

Severe Service Condition

The preceding results were from experiments when the bearing machines ran smoothly. In a few trials, the drive shaft was slightly misaligned. This resulted in service conditions serious enough for severe vibration to be induced. Under such conditions, both the wear index and the maximum percentage area covered were seen to increase with load (Figure 10).

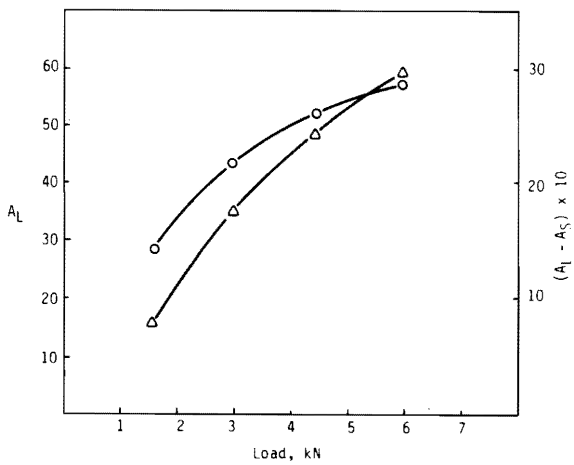

Figure 10. Variation of A_L and $(A_L^2 - A_S^2)$ with Load at 2000 rpm. Bronze Bearings. ○ A_L; △ $(A_L^2 - A_S^2)$.

AUC

The area under the curve, *AUC*, varied linearly with the A_L values. However, considerable scatter resulted when the *AUC* values were plotted against load, although *AUC* increases generally with the bearing surface temperature (Figure 11).

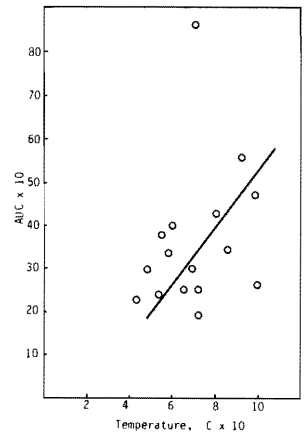

Figure 11. Variation of Area Under the Curve, AUC, with Bearing Temperature. Bronze Bearings.

RESULTS FROM CAST IRON BEARINGS

In the trials with the bronze bearings, wear metal analysis of the oil by AA spectroscopy showed copper, lead and, occasionally, tin. Visual observation of the bronze bearings showed them to wear. Very rarely, however, the ferrograms showed bronze particles. This was expected and the particles examined were therefore from the hard steel sleeves.

A series of trials were next carried out with grey cast iron bearings. (Table 2).

Figure 12 shows the A_L values to increase and

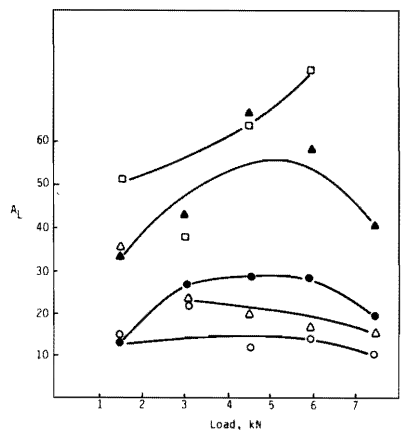

Figure 12. Variation of A_L with Load for Cast Iron Bearings at Various Speeds. rpm: ○ 500; △ 1000; ● 1500; ▲ 2000; □ 2500.

then fall as the applied load gets higher. The results at several speeds are plotted here and are more consistent than those with the bronze bearings. At the speed of 2500 rpm, the cast iron bearing seized when the load was increased to 6 kN and the values are seen to increase at an increasing rate. The area under the curve shows a similar pattern with load (Figure 13) except that the values at 1000 rpm are lower than those at 500 rpm. The A_L values increase with bearing temperature (Figure 14) as do the AUC values (Figure 15). The scatter in this latter case is less than that obtained with bronze bearings.

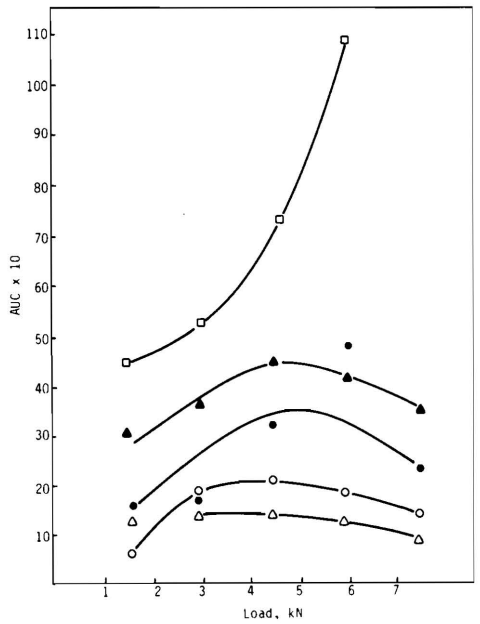

Figure 13. Variation of AUC with Load for Cast Iron Bearings at Various Speeds; rpm: ○ 500; △ 1000; ● 1500; ▲ 2000; □ 2500.

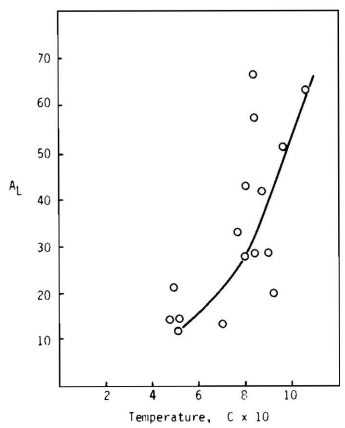

Figure 14. Variation of A_L with Bearing Temperature for Cast Iron Bearings.

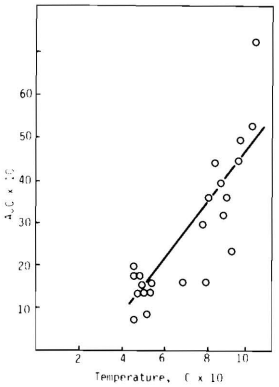

Figure 15. Variation of AUC with Bearing Temperature for Cast Iron Bearings.

There is a trend for the maximum percent area covered to be larger, the higher the interfacial friction. The results are not shown because there was still a lot of scatter.

Wear Debris

The nature of the wear debris on the ferrogram was scrutinized under the ferroscope for all the trials. At the lightest loads and speeds employed, the particles were largely in the form of platelets and there appeared to be a preponderance of oxides. As the load increased, some smaller particles became evident (Figure 16) between thick clusters which could be as much as 400 μm wide. As the speed increased to 2500 rpm, these small particles were noted even at the lightest load employed (1.5 kN) but the clusters became massive.

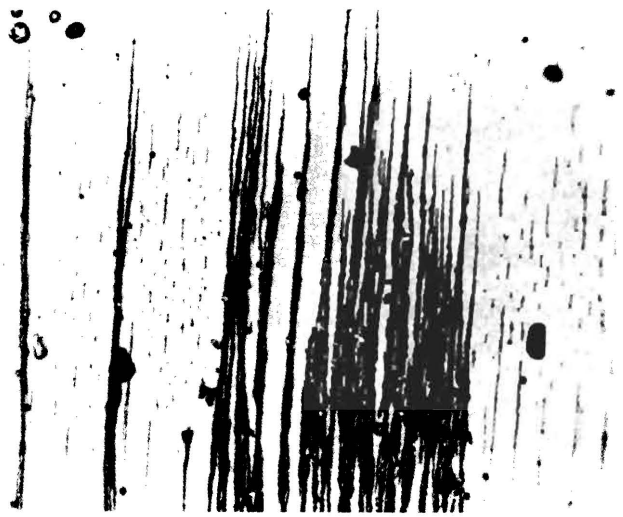

Figure 16. Photomicrograph of Wear Debris on a Ferrogram. D = 54 mm. Bronze Bearings. Load 4.5 kN. Speed 1000 rpm.

Pin-Disc Machine

Some of the results such as a decrease in A_L with load were puzzling. To see if the speculations, as under discussion later, regarding the reasons for these were reasonable, some exploratory work was carried out using a machine where a steel rod 6.25 mm in diameter was loaded against a rotating steel disc. In one series of experiments, the sliding was dry. In another, the interface was lubricated with the same oil as used with the bearing rigs. The oils from the lubricated sliding experiments were used to prepare ferrograms and A_L values were seen to decrease with load (Table 5). The debris from the dry runs was dispersed in oil and the prepared ferrograms showed A_L values to increase generally with load, but not linearly.

Table 5. Weight Loss and A_L Values of 6.25 mm Dia. Steel Pins Run on Steel for 30 Minutes.

Load g	Wt. loss g × 10^{-4}	A_L
300	9	28.6
350	14	31.7
450	26	46.1
550	28	36.7
650	197	81.3
750	221	77.6
Lubricating Sliding		
300	12.3	81.7
500	12.1	85.5
750	12.6	37.3
1000	14.8	20.1

DISCUSSION

In situ measurement of wear of rotary components is not easy and it is not surprising that attempts to do this were unsuccessful in these experiments with the twin bearing rig. However, ferrography is now an accepted technique in condition monitoring of machines on the basis that the history of rotary parts is contained in the size and morphology of the emerging wear particles. Any attempt, therefore, to correlate the percent area of the wear debris with service conditions such as load and speed is worthwhile.

Theoretical considerations show [16] that the radius of a wear particle is proportional to the applied load, W. The area of the wear particle should therefore be proportional to W^2. Taking the results for the bronze bearings at high speeds (Figure 6), the trend is for the area to decrease, taking A_L as a measure of the area of the wear particle. The corresponding results with the cast iron bearings are more consistent and the A_L values tend to increase with load but decrease later.

The annular space between a bearing and its counterface is narrow so that it can not always expel the particles generated at the interface. There was some indirect evidence of this in these experiments when, during a run, the frictional torque tended to rise for a while or the oil pressure built up to fall again as sliding continued. It is reasonable to conclude then that the particles built up to a certain concentration in the annular space between the sleeve and the bearing and became comminuted, escaping to the circulating oil thereafter. The higher the load, the less was the clearance between the bearing and the counterface and the greater the chance for comminution.

As Table 5 shows, for dry runs, where most of the particles escaped from the friction couple, an increase in load gave a high weight loss as expected and the A_L values increased generally. When the sliding was in a lubricating oil, the particles had a chance to return to the interface. It is noted that with increasing load, the weight loss becomes progressively higher but there is a dramatic fall in the A_L values as the load is raised to 750 kg.

The clusters of particles on the ferrogram are close together when the A_L values are high. Since A_L at a particular speed in these experiments decreases with load, the clusters on the corresponding ferrogram should separate into larger number of narrower strips. That is, the N_L values should be high with increasing load. If N_L decreases with increasing A_L, the width, Y_L, should increase with increasing load. However, N_L and Y_L values do not show this logical trend in these experiments. Measurement of N_L or Y_L, therefore, is not a promising area of finding correlation with load or speed for these bearings.

The thickness, h_L, does not show a definitive trend with the service variables. However, like the values of N_L and Y_L, there was considerable scatter. A statistical analysis is necessary but that will have to be an investigation spread over several years considering the time it takes to complete one bearing trial only.

Archard's wear law [17] relates the volume, V, of wear to the applied load, W, and the yield stress, σ_y of the metal as,

$$\frac{V}{S} = K \frac{W}{9\sigma_y} \qquad (5)$$

where, S = sliding distance and K is a probability factor. If v is the sliding velocity and t, the time for a sliding distance, S, equation 5 can be written as

$$V = KvtW/9\,\sigma_y \qquad (6)$$

The dependence of wear volume on the surface speed is thus obvious. Since, in these experiments, the temperature of the bearing rose with the surface speed of the sleeve, the yield stress, σ_y of both members of the friction couple should decrease. In that event, the contacting asperities will yield readily and the areas of contact will be larger, the higher the interfacial temperature. An increase in the value of A_L with temperature is thus promising. This being the case, the use of temperature reached in service as a tool for condition monitoring should be a profitable field for detailed investigation.

Plotting the wear index against load shows a similar pattern to that of A_L. Calculation of the wear index is thus unnecessary and A_L by itself should be an adequate criterion for machine monitoring.

The parameter, area under the curve, AUC, can be regarded as the total volume of the wear particles. Although, with the bronze bearings, AUC did not show a decisive relationship with load, it gives a better correlation with temperature than does A_L.

As Table 4 shows, it was not possible to detect any changes in the properties of the used oil nor was there any significant change in the metals content as analysed by spectroscopy. The likely reason is that within the lifetime of these experiments, the wear volume was low. The experiments with the bronze bearings show clearly that the technique of ferrography is not suitable for nonferrous components even if they are against steel and picking up an amount of ferrous material by metal transfer.

The total wear for most mechanisms is the sum of the wear of each member of the friction couple. When the bearings were bronze, the nonferrous particles remained outside the ferrogram. The slides therefore showed the wear product from the hard steel sleeve only. Since this is not the total volume of wear, scatter of data resulted when experiments were carried out with bronze bearings. Since most of the wear product is expected to be trapped by the ferrograms; cast iron bearings showed more positive trends when A_L values were plotted against load or service temperature. The area under the curve is again a more reliable parameter than A_L.

Looking at the results from both the bronze and cast iron bearings, when the machine ran smoothly, the particle size tended to decrease at heavy loads. The only possible reason is comminution and a suggested physical model of the wear process is as follows.

Initially particles are produced whose size depends on the load and speed. With continuous running, some of the trapped wear particles at the interface become comminuted while a number of large particles escape. The process continues until an equilibrium distribution of particle sizes is established.

If the particle size is large initially, in spite of comminution, large particles predominate in the circulating oil. This is the suggested reason why the A_L values are large when the speed and, hence, the temperature of the sliding interface is increased.

In the present trials, the role of ferrography in condition monitoring of cast iron bearings is encouraging. A machine is running well when it shows minimum vibration and noise. The sliding surfaces are then relatively smooth; the clusters on the ferrogram show widely spaced strips and the A_L or AUC values are low. Vibration results in high values of A_L.

The trials with the cast iron bearings showed that a speed of 2500 rpm was too high for this material. Its yield strength must have lowered substantially for the bearing surface to scuff, resulting in massive transfer of metal onto the sleeve. One could conclude therefore that if a machine shows progressively increasing values of A_L, the warning of imminent seizure is there and steps can be taken to avoid incipient failure. If the machine operates without distress, the A_L values will remain within a range and be relatively low.

CONCLUSIONS

On the basis of the present investigation, the following conclusions are drawn.

1. The parameter, A_L, the maximum percent area

covered, gives the same trend with service variables as does the wear index or the area under the curve. A_L is easier and quicker to measure.

2. When one of the members of the friction couple is non-ferrous, scatter of results is high.
3. Ferrous couples reduce scatter and the results are more consistent.
4. If a machine runs smoothly, A_L increases with speed but does not change dramatically with load. With heavy loads, however, there is the possibility of comminution of the generated wear particles at the sliding interface.
5. If the machine is in distress, A_L increases with load and speed, giving warning of incipient failure.

ACKNOWLEDGEMENTS

It is a pleasure to acknowledge with thanks the financial grant provided by SANCST, The Saudi Arabian National Center for Science and Technology, which made this work possible. The author is grateful to Dr. Fahd H. Dakhil, Vice Rector for Research & Graduate Studies at the University of Petroleum & Minerals for his unfailing support throughout the life of the project. My thanks are also due to Dr. Mansour O. Nazer, Dean of Engineering, for providing laboratory space.

REFERENCES

[1] L. L. Stavinoha and B. R. Wright, 'Spectroscopic Analysis of Used Oil', *National Combined Fuels and Lubricants and Transportation Meetings, Houston, Texas, November 4-7 1969, SAE Paper 690776.*

[2] W. Hoffman, 'Some Experience with Ferrography in Monitoring the Condition of Aircraft Engines', *Wear,* **65** (1981), p. 307.

[3] E. Jantzen, V. Buck, and S. H. Kaegler, 'Influence of Particle Size on Wear Assessment by Spectrometric Analysis', Wear, **87** (1983), p. 331.

[4] M. J. Devine (Ed), *Proceedings of a Workshop on Wear Control to Achieve Product Durability, Naval Air Development Center, Warminster, Pennsylvania, U.S.A.* (1977).

[5] C. W. Chandler Jr., 'An Investigation of the Navy Oil Analysis Program (NOAP) as Applied to Jet Aircraft Engines and Accessories', Naval Aviation Integrated Logistic Support Center, U.S.A. (1976), *NAILSC Report 03-41.*

[6] D. Scott, W. W. Seifert, and V. C. Westcott, 'The Particles of Wear', *Scientific American,* **230** (1974), p. 86.

[7] V. C. Westcott, 'Ferrographic Analysis - Recovering Wear Particles From Machines to Humans', *Naval Research Review,* **30** (1977), p. 1.

[8] W. W. Seifert and V. C. Westcott, 'A Method for the study of Wear Particles in Lubricating Oil', *Wear,* **21** (1972), p. 27.

[9] D. Scott, 'Debris Examination - A Prognostic Approach to Failure Prevention', *Wear,* **34** (1975), p. 15.

[10] D. Scott and G. H. Mills, 'An Exploratory Investigation of the Application of Ferrography to the Monitoring of Machinery Condition from the Gas Stream', *Wear,* **48** (1978), p. 210.

[11] B. J. Roylance, M. H. Jones, and A. L. Price, 'Quantitative Analysis in Ferrography', *Tribology Conference, I. Mech. E (London), at Swansea, Paper No. CHH/78, (1978).*

[12] G. Pocock and P. Gadd, 'The Relationship Between the Ferrogram Entry Deposit and the Iron Content of Used Lubricating Oils', *Wear,* **39** (1976), p. 161.

[13] A. Belmondo, F. Giuggioli, and B. Giorgi, 'Optimisation of Ferrographic Oil Analysis for Diesel Engine Wear Monitoring', *Wear,* **90** (1983), p. 49.

[14] E. D. Yardley and G. Moreton, 'An Attempt to Quantify the Limits of Failure Detection by Ferrography', *Wear,* **90** (1983), p. 272.

[15] V. C. Westcott and W. W. Seifert, 'Investigation of the Iron Content of a Lubricating Oil Using Ferrograph and an Emission Spectrometer', *Wear,* **23** (1973), p. 239.

[16] E. Rabinowicz, 'A Quantitative Study of the Wear Process', *Proceedings of the Physical Society B,* **66** (1953), p. 929.

[17] J. F. Archard, 'Contact and Rubbing of Flat Surfaces', *Journal of Applied Physics,* **24** (1953), p. 981.

Paper Received, 3 March 1985; Revised 5 October 1985.